Proceedings of the IASS 2024 Symposium
Redefining the Art of Structural Design
August 26-30, 2024, Zurich Switzerland
Philippe Block, Giulia Boller, Catherine DeWolf,
Jacqueline Pauli, Walter Kaufmann (eds.)

Mechanical performance and engineering applications of large-span tension-string timber folded plate latticed shell structure

Hua MAO*, Jiemin DING

*College of Civil Engineering, Tongji University
1239 Siping Road, Shanghai, China
mh@tjad.cn

Abstract

The large-span tension-string timber folded plate latticed shell structure is a new type of large-span steel-timber composite structures, which combines the advantages of both the timber folded plate latticed shell structure and the tension-string structure. Based on summarizing the geometric forms of typical folded plate latticed shell structures, the comparative study was conducted on the mechanical performance. And the structural efficiency under different geometric forms was obtained. Based on the above analysis, the study on the tension-strings arrangement of the large-span timber folded plate latticed shell structure was carried out. The influence of tension-string arrangement on the stiffness, stability and ultimate bearing capacity of large-span timber folded plate latticed shell structure has been studied. The influence of joint stiffness on the mechanical performance of setting tension-strings and not setting tension-strings timber folded plate latticed shell structure was analyzed. Based on the above conclusions, the design analysis of the large-span tension-string timber folded plate latticed shell structure was carried out, taking the Anhui Academy of Arts Gymnasium as an engineering case, which provides reference for similar engineering practices.

Keywords: timber folded latticed shell structure, geometric form, structural efficiency, string arrangement, joint stiffness

1. Introduction

In large-span buildings, the beauty of rationality and logic of the structure is increasingly being paid attention to and favored. The folded plate latticed shell structure combines the characteristics of folded plate structure and latticed shell structure. Its naturally formed ridges and valleys not only enrich the aesthetic design of the structure, but also improve the overall stress performance of the structure. It is also convenient for roof drainage and construction. The folded plate latticed shell structure has been increasingly used in large-span buildings.

In terms of materials, compared with steel, which is the most widely used structural material, timber has received more and more attention and application due to its unique aesthetic value, ecological and sustainable advantages, as well as excellent structural performance and process system, especially in the current era where ecological and sustainable development are becoming increasingly important. However, the absolute strength of timber is not high, with low tensile and shear strength, and brittle characteristics in failure. There is a large difference in physical and mechanical properties between the longitudinal and transverse lines, and the transverse strength is low. In addition, the joints of timber structures are limited by the connection mode and performance. Therefore, the application of pure timber structures in large-span engineering is also subject to many limitations. Steel-timber composite structure is a new type of composite structure that not only retains the advantages of timber structure's aesthetics and sustainability, but also fully utilizes the mechanical properties of steel and timber, to achieve the best utilization effect.

2. Folding plate geometry form and structural efficiency

2.1. Folded latticed shell form

Folded latticed shells have various forms and diverse shapes, and their classification methods vary depending on different variables.

There are mainly the following types: (1) Classified by the direction of force on folded plates: unidirectional folded plates, bidirectional or multi-directional folded plates, and composite folded plates; (2) Classified by the characteristics of unit form: single element folded plate shaped latticed shells, multiple element folded plate shaped latticed shells, and composite folded plate shaped latticed shells; (3) Classified by the number of layers of folded plate latticed shells: single-layer folded plate latticed shells, double-layer or multi-layer folded plate latticed shells; (4) Classified by the form of structural planes: rectangular planes, circular planes, circular planes, polygonal planes, etc. In addition, there are variables such as joint connection methods and basic unit systems for classification.

In a typical unidirectional folded plate structure, the geometric shapes of the folded plate at both ends and in the middle can be roughly divided into the following types, as shown in Figure 1: (1) Same direction at both ends and the mid-span; (2) Same direction at both ends, opposite direction at the mid-span; (3) Same direction at both ends, flattened at the mid-span; (4) Reverse both ends. The variation of parameters such as ends and mid span shape, member connection method, ends and mid-span bending depth in each geometric form has a significant impact on the static vertical stiffness and stability performance of the folded plate.

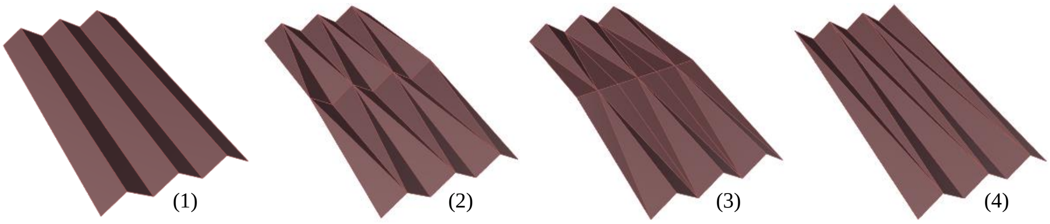

Figure 1: Schematic diagram of folded plate geometry form

2.2. Structural performance

A comparative analysis model of geometric forms was established in combination with practical engineering. There are a total of 5 models with different geometric forms, as shown in Figure 2 and Table 1. The model parameters are detailed in Table 2, and the design indicators for material labeling are taken according to Chinese design standards. In these models, the two ends of main beams (the ridge and valley beams), are rigidly connected, and the two ends of the secondary beams are hinged.

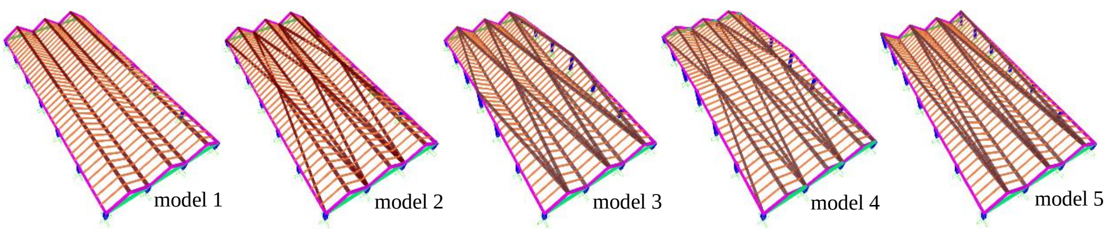

Figure 2: Geometric form of the models

Table 1: Description of the models

Model 1	Both ends in the same direction, mid-span in the same direction, no diagonal braces
Model 2	Both ends in the same direction, mid-span in the same direction, set diagonal braces
Model 3	Both ends in the same direction, mid-span reverse
Model 4	Both ends in the same direction, mid-span flattening
Model 5	Both ends reverse

Table 2: Basic parameters of the models

Timber grade	TC_T32	Steel grade	Q355B
Span (m)	54	Column spacing (m)	8.5
Rise (m)	3	Secondary beam spacing (m)	2.5
Section of ridge and valley beam (mm)	700×300	Section of secondary beam (mm)	300×200
Section of steel edge beam (mm)	B600×600×14×20	Section of steel column (mm)	B600×600×30×30
Dead load DL (kN/m^2)	1.0	Live load LL (kN/m^2)	0.5

The vertical deformation nephograms, vertical displacements, eigenvalue buckling factors, and maximum internal forces under the action of 1.0DL+1.0LL(all comparative analyses are considered based on this load combination) are shown in Table 3, where the maximum internal forces is taken from the main beams.

Table 3: Calculation results of different geometric forms models

Model No.	1	2	3	4	5
Deformation nephogram	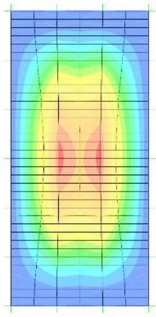	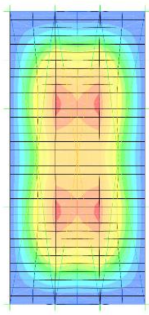	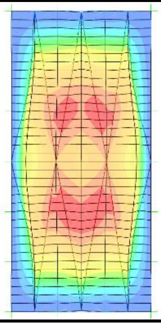	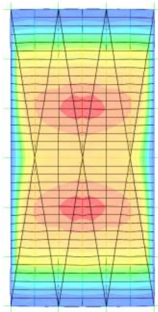	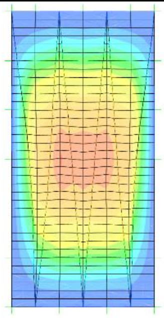
Vertical displacement at mid-span Δ_{mid} (mm)	2277	208	206	143	1420
Maximum vertical displacement Δ_{max} (mm)	2277	267	234	180	1420
Eigenvalue buckling factor γ	4.77	9.61	10.4	11.7	5.02
Maximum axial force F_{max} (kN)	496	1291	1880	808	548
Maximum bending moment M_{max} (kN·m)	3453	1181	1153	552	3164
Maximum shear force V_{max} (kN)	780	369	452	155	946

According to the analysis results, it can be seen that models 1 and 5 are deformed and subjected to forces similar as single span beams, with weak stiffness and large component bending moments. Model 5, due to the formation of a diagonal beam with opposite ends, a portion of the vertical load is transmitted through axial force. At the same time, the spatial effect is increased, and the vertical stiffness and stability performance are improved. The maximum bending moment is reduced by about 10%, and the maximum axial force and shear force are increased by about 10% and 20%, respectively. Models 2, 3, and 4, due to the height difference between the mid-span and two end supports, form an arched folded beam in the main beam. Therefore, their stress performances are significantly different from models 1 and 5. The force mechanism is similar to that of a double span continuous beam symmetrical with elastic supports at the mid-span. The maximum vertical deformation is significantly reduced and does not occur at the mid-span, and the stability performance is significantly improved. The maximum bending moment and shear force of the main beams in models 2, 3, and 4 are significantly reduced, while the maximum axial force increases. The force form of the main beam changes from a beam type force dominated by bending to an arch type force dominated by axial compression. This helps timber to fully utilize its axial compression performance, reduce its bending and shear, and maximize its mechanical properties.

In summary, by utilizing the geometric form of folded plates and the height difference between ridges and valleys, the main beam can form an arched folded beam, which can greatly improve the stiffness and stability of the folded plate latticed shell. At the same time, the stress on the components can also fully utilize the higher axial compression capacity of timber. The arch folding beam of Model 4 has the strongest effect and the most significant effect. The following parameter analysis will be conducted based on Model 4.

2.3. Rise

According to the previous analysis, rise is a key parameter of the folded plate lattice shell structure, which is composed of the end bending depth and the central lifting height, as shown in Figure 3.

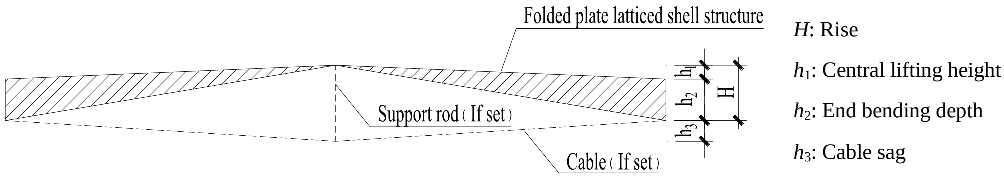

Figure 3: Schematic diagram of model geometric parameters

Without considering the central lifting (i.e. h_1=0), the mechanical performance of folded plate lattice shell structures with rise of 2m, 3m, 4m, 5m, and 6m, i.e. rise to span ratios of 1/27 to 1/9, is compared. The results are shown in Table 4. The curve of maximum vertical displacement with rise is shown in Figure 4. The curve of eigenvalue buckling factor with rise is shown in Figure 5.

Table 4: Calculation results for different rises

Rise H (m)	2	3	4	5	6
Maximum vertical displacement Δ_{max} (mm)	278	180	142	127	119
Eigenvalue buckling factor γ	9.73	11.7	13.1	13.8	14.2
Maximum axial force F_{max} (kN)	1085	808	717	672	637
Maximum bending moment M_{max} (kN·m)	663	552	516	487	470
Maximum shear force V_{max} (kN)	147	155	161	166	169

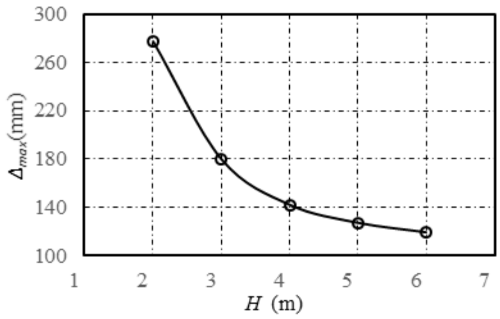

Figure 4: The curve of Δ_{max} with H

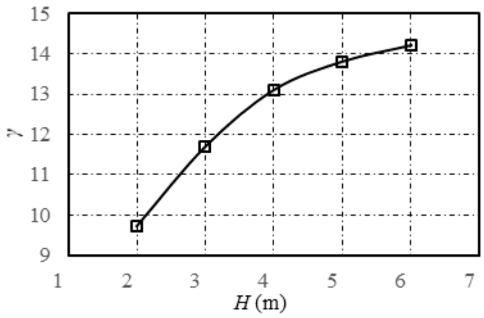

Figure 5: The curve of γ with H

The analysis results indicate that the vertical stiffness and stability performance of folded plate lattice shell structure increase with the increase of rise, but the rate of increase gradually slows down. The maximum axial force and maximum bending moment of the main beams decrease with the increase of rise, while the maximum shear force remains almost unchanged. As the rise increases, the effect of arch increases. When the rise to span ratio is less than 1/18, the effect of rise on stiffness and stability is significant. When the rise to span ratio is greater than 1/12, the effect gradually weakens. The rise of the folded grid shell structure should be taken as 1/18 to 1/12 of the span.

2.4. Central lifting height

The force performance of folded plate lattice shell structures with a central lifting height of 0, 1, 2, and 3 meters and the rise of 4 meters is compared below. The results are shown in Table 5. The curve of maximum vertical displacement with central lifting height is shown in Figure 6. The curve of eigenvalue buckling factor with central lifting height is shown in Figure 7.

Table 5: Calculation results for different Central lifting height

Central lifting height h_1 (m)	0	1	2	3
Maximum vertical displacement Δ_{max} (mm)	142	136	131	127
Eigenvalue buckling factor γ	13.1	13.5	13.7	13.8
Maximum axial force F_{max} (kN)	717	835	703	678
Maximum bending moment M_{max} (kN·m)	516	521	508	490
Maximum shear force V_{max} (kN)	161	143	131	126

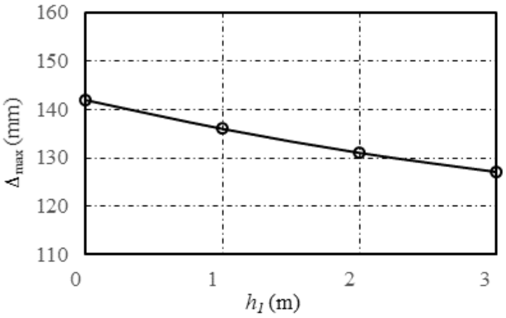

Figure 6: The curve of Δ_{max} with h_1

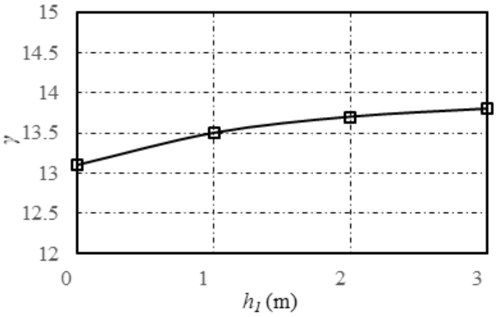

Figure 7 The curve of γ with h_1

The results indicate that when the rise remains constant, the vertical stiffness and eigenvalue buckling factor of the structure will increase with the increase of central lifting height, but the impact is not significant. The distribution of internal forces in components does not vary significantly under different central lifting height. In summary, the main factor affecting the mechanical performance of folded plate lattice shells is the rise to span ratio. When the rise to span ratio is constant, changing the ratio of end bending depth and central lifting height will not greatly affect the structural efficiency of folded plate lattice shells.

2.5. Joint stiffness

The joints of timber structures generally show semi-rigid characteristics, and their stiffness values are a key part of timber structure design. Using model 4 with a rise of 4m and a central lifting height of 1m, the stiffness coefficients of the joints at both ends and mid-span of the main beam are set to 0, 0.2, 0.4, 0.6, 0.8, and 1, respectively, to explore the influence of joint stiffness on the stress performance. The stiffness coefficient is the ratio of the bending stiffness of joint to the bending stiffness of joint's rigid connection, where 0 represents hinge connection and 1 represents rigid connection. The results are shown in Table 6. The curve of maximum vertical displacement with joint stiffness coefficient is shown in Figure 8. The curve of eigenvalue buckling factor with joint stiffness coefficient is shown in Figure 9.

Table 6: Calculation results for different joints stiffness coefficients

Joint stiffness coefficient K/K_{rigid}	0	0.2	0.4	0.6	0.8	1.0
Maximum vertical displacement Δ_{max} (mm)	218	172	158	149	142	136
Eigenvalue buckling factor γ	7.61	11.2	12.3	12.8	13.2	13.5

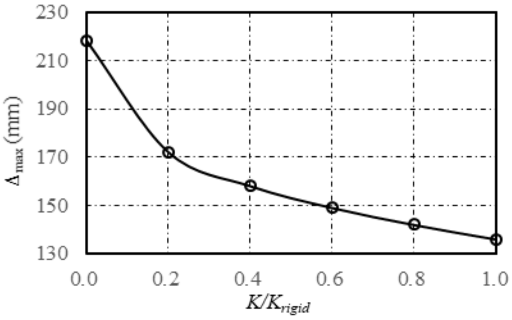

Figure 8: The curve of Δ_{max} with K/K_{rigid}

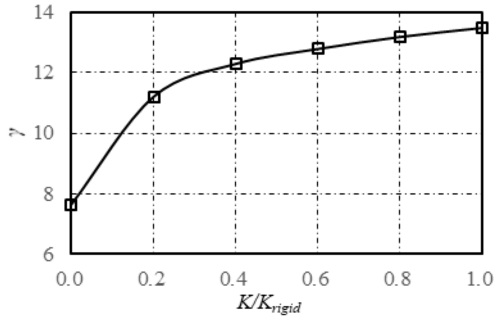

Figure 9: The curve of γ with K/K_{rigid}

From the results, it can be seen that the folded plate lattice shell structure is relatively sensitive to changes in joint stiffness. Compared with rigid joints, hinged joints increase the maximum vertical displacement by 60% and reduce the eigenvalue buckling factor by 44%. When the joint stiffness coefficient gradually increases from 0 (hinged), the maximum vertical deformation decreases rapidly, the eigenvalue buckling factor increases rapidly, and the amplitude gradually slows down. For safety reasons in engineering, timber components are often calculated based on hinge joints at both ends, which is conservative. It is recommended to conduct joint tests or finite element analysis, and consider joint stiffness appropriately.

3. Cable arrangement

In large-span timber structure engineering, due to some factors such as the structural performance and cost of timber structures, tension strings are often used to improve the static stiffness and stability, adjust the distribution of internal forces, and increase the ultimate bearing capacity of structure. This chapter introduces the cable and strut system to explore the effects of different cable sags on structural performance, and further explores the influence of tension strings on the vertical stiffness and ultimate bearing capacity under different joint stiffness. The results are compared with those of the previous chapter without the arrangement of tension string structures.

In this chapter, the geometric nonlinearity of structure is considered when calculating the ultimate bearing capacity of the folded plate lattice shell. The uniform defect method is used to introduce defects, and the first buckling mode obtained from the linear buckling analysis of the structure is taken as the initial defect. The maximum initial defect of the structure is taken as 1/300 of the span, and the arc length method is used to conduct a full process equilibrium path tracking analysis of the structure.

3.1. Cable sag

The cable sag (see Figure 3) is an important factor affecting the efficiency of the tension strings structure. Considering the cable sags of 0, 0.5m, 1m, 1.5m, and 2.0m, the analysis results are shown in Figures 10 and 11.

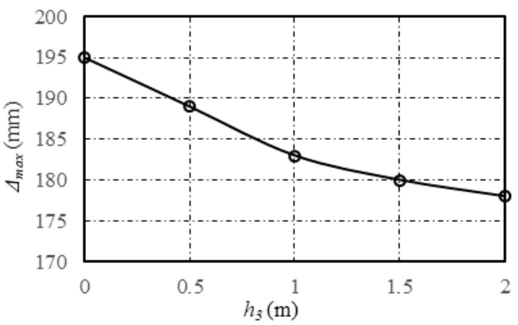

Figure 10: The curve of Δ_{max} with h_3

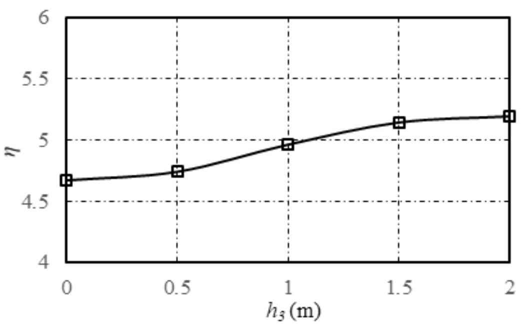

Figure 11: The curve of γ with h_3

As shown in the figure, the cable sag has a significant impact on the vertical stiffness of the structure. Increasing the cable sag appropriately can effectively improve the vertical stiffness of the structure. This is because increasing the cable sag will lead to a smaller angle between the cable and the support rod, which increases the vertical resistance force and reduces the vertical displacement. The increase in cable sag will also increase the ultimate bearing capacity of folded plate lattice shell structure, but the extent of improvement is relatively limited. When the cable sag is greater than 1.5m, that is, when the sag to span ratio is greater than 1/36, the increase in cable sag will hardly increase the ultimate bearing capacity of the structure.

3.2. Joint stiffness

The comparative results of setting and not setting cables on the stiffness and ultimate bearing capacity of timber folded plate lattice shell structures under different joint stiffness are shown in Figure 12 and Figure 13.

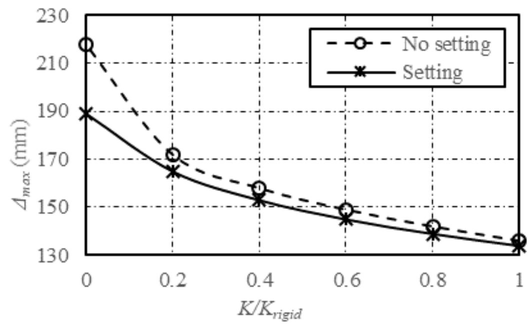

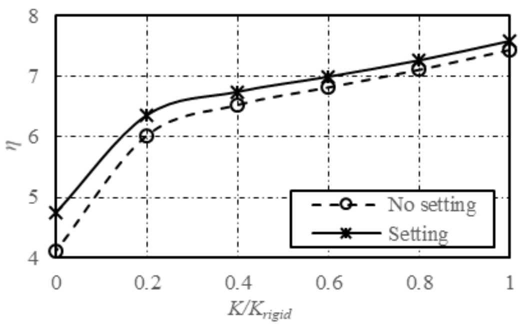

Figure 12: The comparison of Δ_{max} with K/K_{rigid}

Figure 13: The comparison of Δ_{max} with K/K_{rigid}

The results indicate that the weaker the stiffness of upper folded plate lattice shell structure, the more effective the improvement of tension strings on stiffness and ultimate bearing capacity. When the main beam joints are hinged, the stiffness increases by about 13% and the ultimate bearing capacity increases by about 15%. At the same time, tension strings can reduce the sensitivity of the structure to joint stiffness. Comparing the results of joint hinge and rigid connection, after setting cables, the sensitivity of the maximum vertical displacement and ultimate bearing capacity to joint stiffness is reduced by about 32% and 16%, respectively.

4. Engineering applications

4.1. Project profile

The Anhui Academy of Arts Gymnasium has a longitudinal length of 51m, a span of 54m, and a column spacing of 8.5m. According to the requirements of the architectural form and effect, the roof adopts a timber folded plate latticed shell structure.

4.2. Structural system and joint Design

A comparison was made on the structural system using the method shown above. Combine the architectural design, the rise of the folded plate lattice shell structure is determined to be 4 meters, with a central lifting height of 1 meter, and a one-way cable is set. On this basis, the schemes without diagonal bracing, single diagonal bracing and double diagonal bracing at the end are compared. The results show that both the single and double diagonal bracing schemes can improve the bending moment of the main members at the ends and mid-span. Considering the convenience of member joint installation, the single diagonal bracing scheme is adopted. Steel ring beams are installed at the boundary of the roof to improve the peripheral stiffness and anchoring effect of the structure.

In joint design, to avoid section weakening and stress concentration caused by the intersection of timber components, and to ensure the stiffness of joint connections, steel joints, embedded steel plates and high-strength bolts are used. The joint design fully considers the appearance and reliability of the structure, optimizes the joint, and shifts the joint partition inward to reduce the size of the joint.

Figure 14 shows the structural system of the roof, and Figure 15 shows the typical joint composition and 3D printed model. It’s the roof central ridge beams joint, which has 6 main beams, 2 secondary beams and 2 diagonal braces connected. It is the most complex joint in the project.

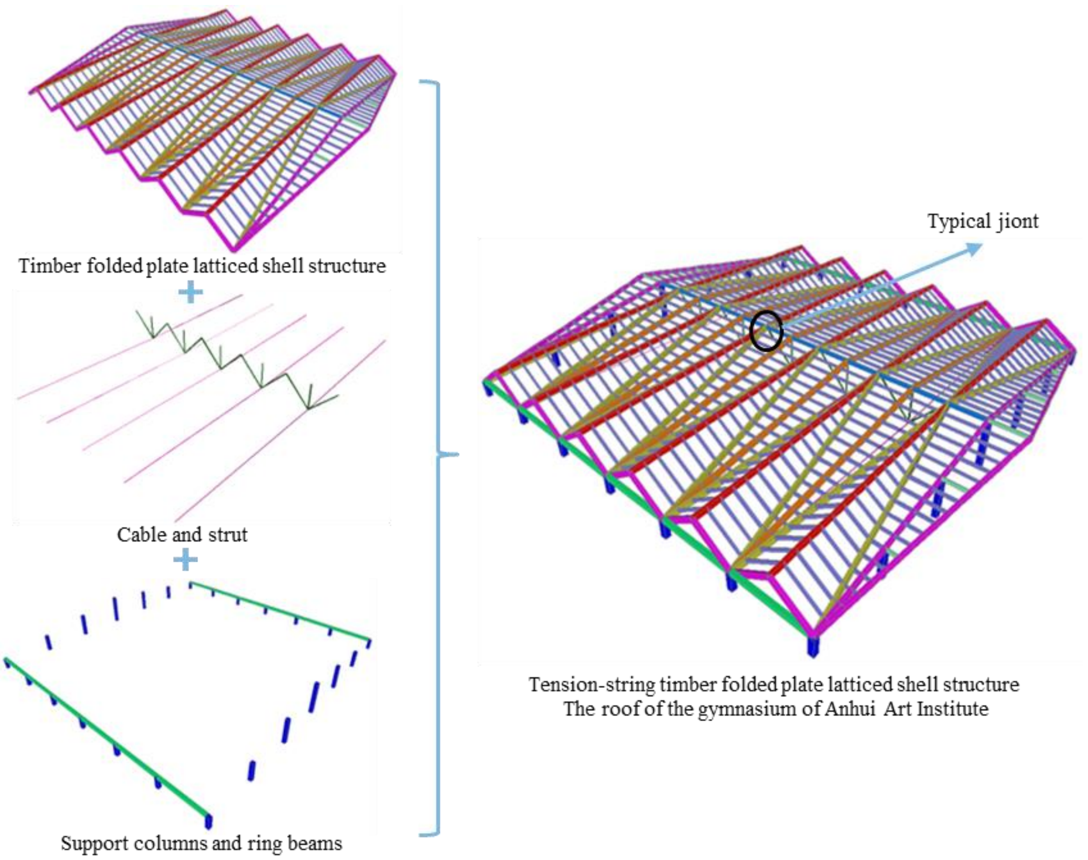

Figure 14: Roof structural system diagram

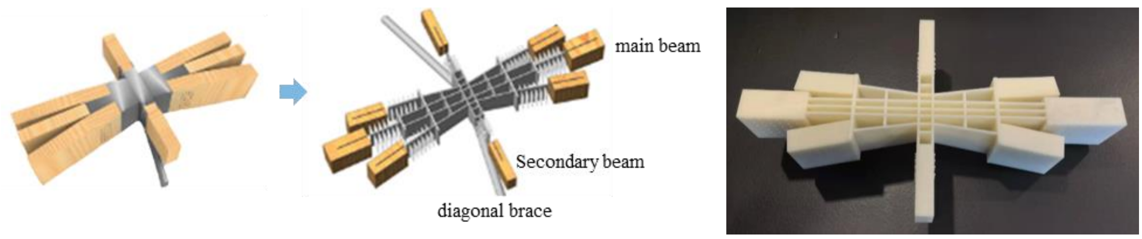

Figure 15: Typical joint composition diagram and 3D printed model

4.3. Analysis results

The structure was analyzed using SAP2000 for various loads and effects combinations. Buckling and ultimate bearing capacity analysis were also conducted. Under the combined action of vertical loads, considering the adverse effects of uneven distribution of live or snow loads, the maximum deflection of the structure is 177.1mm, which is 6% more than the full span uniformly distributed live load arrangement. The deflection to span ratio is 1/305, meeting the requirements of the codes. The first period of the structure is 0.629 seconds, and the vibration mode is the overall anti symmetric vertical vibration of the roof structure. The first six vibration modes are all vertical vibrations of the roof, indicating that the structure is designed reasonably and has strong anti-torsion ability. The eigenvalue buckling factor is 7.53, and the mode is single wave antisymmetric buckling. The ultimate bearing capacity factor is 6.7, indicating good stability and meeting the requirements of the codes. The maximum stress ratio of timber components is 0.87, mainly at the mid-span and at the connection of surrounding steel columns. It is controlled by a combination of snow loads in vertical loads, and horizontal seismic and wind effects do not have a controlling effect on timber components.

5. Conclusion

1. For typical unidirectional folded plate latticed shell structures, the geometric shape has a significant impact on the mechanical properties of the structure. By utilizing the height difference of the folded plate, one or more elastic support points are formed at the mid span, forming an arched folded beam for the main beam, which can significantly improve the stiffness and stability of the folded plate latticed shell.

2. Rise is a key parameter of the folded plate latticed shell structure. With the increase of rise, the vertical stiffness and stability performance of the folded plate latticed shell structure are improved, the axial force of the main components increases, and the bending moment decreases, which can better utilize the mechanical properties of timber. Analysis shows that when the rise to span ratio is less than 1/18, the effect of rise on stiffness and stability is significant. When the rise to span ratio is greater than 1/12, the effect gradually weakens. The rise of the folded plate latticed shell structure should be taken as 1/18 to 1/12 of the span. When the rise remains constant, the ratio of end bending depth to central lifting height has a relatively small impact on the structural efficiency of the folded plate latticed shell structure.

3. The folded plate latticed shell structure is sensitive to joint stiffness. For safety reasons in engineering, timber components are often calculated based on hinge joints at both ends, which is conservative. It is recommended to conduct joint tests or finite element analysis, and consider joint stiffness appropriately.

4. Setting cables can effectively increase the vertical stiffness and ultimate bearing capacity of folded plate latticed shell structures, and the weaker the stiffness of the upper structure, the more obvious the effect.

5. Setting cables can reduce the sensitivity of the timber structure stiffness, and can reduce the structural safety impact caused by changes in temperature and humidity, joint stiffness, creep, and other factors, providing necessary safety reserves for timber structures economically.

References

[1] Y. Zhang, J Ding and Z. Zhang, "Application features and practice of large span steel-wood composite structures," *Architectural Technique*, no. 11, pp. 14-20, 2018.

[2] Y. Zeng, "Research on mechanical performance of the large-span steel-wood tension-string folded plate structure," *Tongji University*, 2023.

[3] W. Yang, "Construction and shape of folded plate structure," *Harbin Engineering University*, 2005.

[4] S. Wang, "Study on static and dynamic performance of the double table-flap latticed shell structure," *Henan University*, 2011.

Proceedings of the IASS 2024 Symposium
Redefining the Art of Structural Design
August 26-30, 2024, Zurich Switzerland
Philippe Block, Giulia Boller, Catherine De Wolf,
Jacqueline Pauli, Walter Kaufmann (eds.)

Copyright Declaration

Before publication of your paper in the Proceedings of the IASS Annual Symposium 2024, the Editors and the IASS Secretariat must receive a signed Copyright Declaration. The completed and signed declaration may be uploaded to the EasyChair submission platform or sent as an e-mail attachment to the symposium secretariat (papers@iass2024.org). A scan into a .pdf file of the signed declaration is acceptable in lieu of the signed original. In the case of a contribution by multiple authors, either the corresponding author or an author who has the authority to represent all the other authors should provide his or her address, phone and E-mail and sign the declaration.

Paper Title: _ Mechanical performance and engineering applications of large-span tension-string timber folded plate latticed shell structure _

Author(s): _ Hua MAO, Jiemin DING _

Affiliation(s): _ College of Civil Engineering, Tongji University _

Address: _1239 Siping Road, Shanghai, China _

Phone: _0086-21-35375559_

E-mail: _ mh@tjad.cn _

I hereby license the International Association for Shell and Spatial Structures to publish this work and to use it for all current and future print and electronic issues of the Proceedings of the IASS Annual Symposia. I understand this licence does not restrict any of the authors' future use or reproduction of the contents of this work. I also understand that the first-page footer of the manuscript is to bear the appropriately completed notation:

Copyright © 2024 by <name(s) of all of the author(s)>
Published by the International Association for Shell and Spatial Structures (IASS) with permission

If the contribution contains materials bearing a copyright by others, I further affirm that (1) the authors have secured and retained formal permission to reproduce such materials, and (2) any and all such materials are properly acknowledged by reference citations and/or with credits in the captions of photos/figures/tables.

Printed name: _ Hua MAO _ Signature: Hua Mao 毛华

Location: _ Shanghai, China _ Date: _June 27,2024_